Nonplanarity of Adenine: Vibrational Transition Moment Angle Studies in Helium Nanodroplets

Myong Yong Choi,*,† Feng Dong,§ Sang Woo Han,† and Roger E. Miller‡,⊥

Department of Chemistry and Research Institute of Natural Science, Gyeongsang National University, Jinju 660-701, Korea, and Department of Chemistry, The University of North Carolina at Chapel Hill, Chapel Hill, North Carolina 27599

Received: February 12, 2008; Revised Manuscript Received: May 1, 2008

Mid-infrared spectra are reported for adenine monomer in helium nanodroplets. We show that there is only one tautomer of adenine, the global minimum structure, observed in helium nanodroplets and characterized by using ab initio calculations and the measurement of vibrational transition moment angles (VTMAs) for the various vibrational modes of the adenine monomer. On the basis of the VTMA analysis on the amino group of the global minimum tautomer, which gives insights into its nonplanarity, a detailed VTMA study of three lowest-energy amino tautomers of adenine is discussed in this study.

Introduction

Although nucleic acid bases (NABs) are well-known as the building blocks of life,[1,2] the detailed structure of isolated NABs still remains to be solved. NABs were believed to be perfectly planar for many years, until the predictions of nonplanarity of the amino group on the NABs in the early 1990s.[3–8] Hobza and co-workers[4–6] conducted a series of ab initio studies on the nonrigidity of NABs and showed that the nonplanar structure was indeed more stable than the planar structure. Other evidence also supports nonplanarity,[3,9,10] which is caused by the partial sp^3 hybridization of the amino group nitrogen atom.[4,7] Although a large inertial defect of adenine was observed in a microwave study,[11] its cause was not directly related to the nonplanarity of adenine. Unfortunately, due to the experimental difficulties associated with the isolation of single molecules as well as insufficient experimental spectral resolutions, no direct experimental evidence for the nonplanarity of isolated NABs has been provided.

Recently, Dong et al. have provided an unambiguous conclusion on the nonplanarity of the global minimum tautomer of adenine[12] using a recently developed method called vibrational transition moment angles (VTMAs)[12–19] and showed also that these VTMAs are highly dependent on the molecular structure and are rather insensitive to the basis sets used in the ab initio calculations.

In this paper, we report a more complete VTMA study of the three lowest-energy tautomers of adenine (see Figure 1). The nonplanarity is based on the dihedral angle measurements of the amino group with respect to the VTMA changes of the N−H and NH_2 asymmetric and symmetric stretching (AS and SS) vibrational modes in each tautomer.

Experimental Techniques

The infrared spectrum of isolated adenine was carried out by solvating adenine in liquid helium nanodroplets. The experimental apparatus has been described elsewhere in detail;[19,20] thus, only a brief explanation is provided in this paper. Superfluid helium droplets have been shown to be an ideal spectroscopic matrix,[19,21–23] resulting in high-resolution spectra completely devoid of hot bands and vibrational frequencies unperturbed from those in the gas phase. Nanodroplets with a mean size of 3000 helium atoms were formed by expanding ultrahigh-purity helium (99.9999%) from a 5 μm diameter orifice, operated at 50 atm of pressure and a temperature of 20.5 K. Adenine was doped to the droplets by pick-up[24] in a scattering-box oven, the temperature of which was optimized for the capture of a single molecule (∼175 °C). Upon being captured by the droplets, adenine was quickly cooled to the 0.37 K temperature of the droplets.[25,26]

In this work, improved signal levels have been obtained by using a 70 mW periodically poled lithium niobate optical

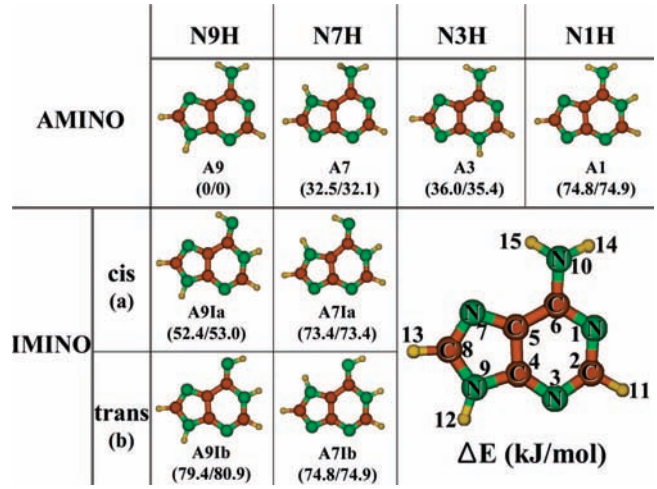

Figure 1. The ab initio structures and relative energies [MP2/6-311++G(d,p)] of the various tautomers of adenine. Amino and imino are classified by certain functional groups in the position of N10, namely, NH_2 and NH, respectively. In addition, the imino forms have two rotational orientations of the NH group, which are cis (a form) and trans (b form) to the five-membered ring. The values in the brackets give the energies relative to A9 in kJ/mol with/without a harmonic zero-point energy correction. Only the global minimum tautomer is experimentally observed in the present study.

* To whom correspondence should be addressed: E-mail: mychoi@gnu.kr.
† Gyeongsang National University.
⊥ The University of North Carolina at Chapel Hill.
§ Present address: Los Gatos Research, Inc., Mountain View, CA 94041
‡ Deceased. November 6, 2005.

10.1021/jp8012688 CCC: $40.75
Published on Web 07/11/2008

TABLE 1: A Summary of the Experimental and Calculated Vibrational Frequencies and VTMAs for the Various Tautomers of Adenine

tautomer	harm. freq. (cm^{-1})	scaled[a] freq. (cm^{-1})	exp. freq. (cm^{-1})	IR. intensity (km/mol)	assignment	ab initio[b] VTMAs (degree)	exp.[c] VTMAs (degree)	dipole moment (Debye)	relative[d] energy (kJ/mol)
A9								2.8	0.0
	3733.7	3573.6	3568.2	52.7	NH_2 AS	21	24		
	3666.4	3509.2	3509.2	112.8	N9H	59	63		
	3602.3	3447.9	3451.6	73.7	NH_2 SS	76	77		
A7								6.7	32.1
	3686.5	3528.4	−	32.5	NH_2 AS	61	−		
	3667.7	3510.5	−	85.3	N7H	15	−		
	3570.9	3417.9	−	37.0	NH_2 SS	54	−		
A3								4.1	35.4
	3740.9	3580.5	−	67.3	NH_2 AS	11	−		
	3608.3	3453.7	−	45.4	N3H	79	−		
	3603.0	3448.5	−	178.5	NH_2 SS	88	−		
A1								8.6	74.9
	3686.6	3528.6	−	45.5	NH_2 AS	39	−		
	3619.6	3464.4	−	84.3	N1H	21	−		
	3569.0	3416.0	−	66.6	NH_2 SS	62	−		
A9Ia								3.9	53.0
	3660.6	3503.7	−	108.9	N9H	14	−		
	3611.7	3456.9	−	76.0	N1H	57	−		
	3533.7	3382.2	−	25.1	N10H	19	−		
A9Ib								4.6	73.4
	3664.0	3506.9	−	108.3	N9H	52	−		
	3619.4	3464.2	−	46.0	N1H	78	−		
	3493.2	3343.4	−	7.9	N10H	7	−		
A7Ia								3.4	90.9
	3662.1	3505.1	−	84.0	N7H	12	−		
	3612.7	3457.8	−	74.4	N1H	88	−		
	3545.8	3393.8	−	13.6	N10H	41	−		
A7Ib								3.8	74.9
	3653.8	3497.1	−	110.0	N7H	57	−		
	3623.3	3468.0	−	49.0	N1H	48	−		
	3512.1	3361.6	−	10.4	N10H	36	−		

[a] The ab initio calculations were performed at the MP2/6-311++G(d,p) level, and the scaled frequencies were obtained by multiplying the harmonic frequencies by a factor of 0.95713. [b] The typical dependence of the ab initio VTMAs on the basis sets is ±1−2°.[16,19] [c] Normal experimental error is within ±5−7°.[16,19] [d] The energy was obtained with zero-point energy correction.

parametric oscillator (cw-PPLN-OPO)[27,28] IR laser from Linos Photonics. The signal was further enhanced by the use of a multipass cell.[20] Vibrational excitation of the solvated molecules resulted in the evaporation of several hundred helium atoms. The resulting laser-induced decrease in the energy of the droplet beam was detected by a bolometer,[29] which was positioned downstream of the laser interaction region. The laser beam was amplitude modulated, and a phase sensitive detection of the bolometer signal was used to improve the signal-to-noise ratio. A series of external etalons and a wavemeter were used to calibrate the resulting infrared spectra.

Measurements of VTMAs and ab Initio Calculations. The pendular-state spectroscopic method has been applied previously to both gas-phase[30–34] and helium nanodroplet[31,35–37] studies. A large direct current (DC) electric field applied between the Stark electrodes results in the orientation of the permanent dipole moment of the molecule parallel to the electric field, in the limit where μE is large compared to the rotational temperature of 0.37 K.[25,26] For a linearly polarized laser, the result will be a change in the excitation efficiency, given that the molecular transition moments will also be oriented in the laboratory frame of reference. If the laser electric field is aligned parallel (perpendicular) to the DC electric field (referred to here as parallel and perpendicular polarization alignments), the corresponding change in the vibrational band intensity will depend upon the angle between the permanent dipole axis and the corresponding transition moment direction. This angle is referred to as the vibrational transition moment angle or VTMA. For a vibrational mode in which the angle between the transition moment and the permanent dipole moment is less than the magic angle (54.7°), a parallel polarization scan will result in an increase in the band intensity, and vice versa for the perpendicular polarization scan, compared to the corresponding band in the zero-field scan. A quantitative description of this effect requires that the orientation distribution for the permanent dipole moment be known. This distribution depends upon the magnitude of the dipole moment, the applied electric field, the rotational constants, and the temperature of the molecule. The methods for calculating this distribution have been discussed in detail previously.[38–40] This distribution is dependent upon the detailed rotational structure in the band, which is, in turn, dependent upon the rotational temperature. However, since the present experimental spectra are broadened beyond the rotational contour, the sensitivity of the orientation distribution to the rotational constants is rather small. As a result, we find that the ab initio rotational constants, divided by a factor of 3 to approximately account for the effects of the helium,[41] can be used to determine accurate VTMAs. This is largely the result of the fact that the rotational temperature is well-determined in these experiments (namely, the droplet temperature of 0.37 K). A detailed discussion of how the experimental VTMAs are extracted from the integrated areas of the zero field parallel and perpendicular polarization spectra is given elsewhere.[13–17,19]

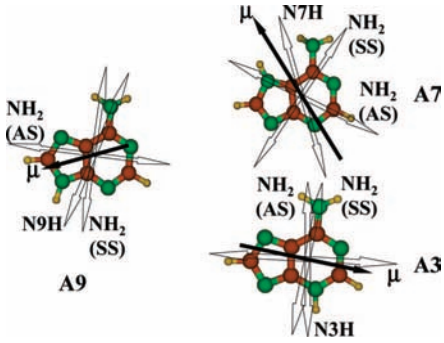

Figure 2. The three lowest-energy tautomers of adenine, showing the corresponding directions of the permanent electric dipole moments (the length of the solid arrow is proportional to the dipole magnitudes) and the vibrational transition moments (empty double ended arrows) for the various vibrational modes. The magnitudes of these moments are given in Table 1.

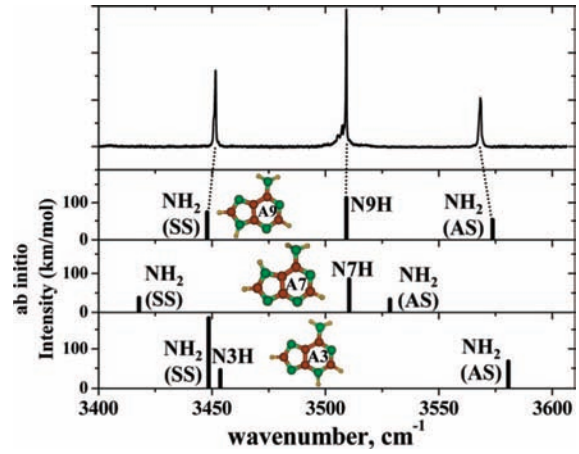

Figure 3. A survey spectrum of adenine in helium droplets. The ab initio vibrational spectra for the three lowest-energy tautomers of adenine are shown in separate panels below the experimental spectrum. The vertical bars in the bottom panels summarize the ab initio frequencies and intensities for the NH_2 (AS), N9H (N7H for A7 and N3H for A3), and NH_2 (SS) stretch modes of the various tautomers. The harmonic ab initio calculations were all scaled by a factor of 0.95713 with a MP2/6-311++G(d,p) basis set to obtain the best overall agreement between theory and experiment, particularly for the free N9H stretch of the A9 tautomer. The dotted lines are meant as a guide to assign the bands associated with calculated frequencies of each vibrational band of A9.

Although the recent systematic theoretical studies[42–45] on the tautomers of adenine have focused on the energetics of the various tautomers of adenine, the information about the permanent dipole and transition dipole directions needed for the comparison with the experimental VTMAs has never been reported. Therefore, we conducted ab initio calculations for the eight amino and imino tautomers of adenine (shown in Figure 1), of which the three lowest-energy amino tautomers (A9, A7, and A3) were extensively studied for the VTMA analysis in this study. Figure 1 shows the eight tautomers of adenine with their relative equilibrium energies listed in brackets (kJ/mol), with/without harmonic zero-point energy corrections at the MP2/6-311++G(d,p) basis set using Gaussian 03.[46] Detailed information about the ab initio VTMAs of the tautomers in Figure 1 is listed in Table 1. The ab initio transition moment vectors (empty double-ended arrows) and permanent electric dipole moments (solid arrows) for the three lowest-energy tautomers which are superimposed on the molecules are shown in Figure 2. The density functional theory calculations (DFT) at Becke's three parameters hybrid functional method (B3LYP) have also been applied for comparison, which will be discussed below.

Results and Discussions

The upper panel in Figure 3 shows an experimental spectrum of adenine in helium nanodroplets that spans the regions corresponding to the NH_2 (AS), N−H, and NH_2 (SS) modes. The lower panels, from the second to the fourth, show the ab-initio-predicted spectra (all scaled by a factor of 0.95713 with a 6-311++G(d,p) basis set) for the three lowest-energy tautomers, A9, A7, and A3, respectively. The assignment of this spectrum is quite straightforward because the vibrational bands are widely separated. Indeed, the ab initio frequencies give a convincing assignment, as guided by the dotted lines in Figure 3. However, even here, some frequency differences between the experimental and scaled calculations still exist, illustrating the difficulties that can arise in assigning vibrational spectra of more complicated molecules, where the spacing between vibrational levels can be smaller than the typical accuracy of the calculations.[14–19] Given that the assignments of the vibrational bands in adenine are well-established, it has served as an excellent test case for illustrating the use of the present method for measuring VTMAs.[12]

Figure 4 shows the expanded regions of the NH_2 (SS), N9H, and NH_2 (AS) modes of the A9 tautomers, recorded with (a) an applied DC electric field directed parallel, (b) no applied field, and (c) perpendicular (electric field being 80 kV/cm) to the laser polarization direction for each vibrational band. Using the methods discussed elsewhere,[12,14–19] we made use of the integrated areas under the corresponding peaks to determine experimental VTMAs for the NH_2 (SS) band at 3451.6 cm^{-1}, namely, 77°, which is in excellent agreement with the ab initio value of 76° (normal experimental error being within ±5−7°).[16,19] The other two bands, labeled α and β in Figure 4, which disappear at lower oven temperatures (Figure S1 shown in the Supporting Information), are assigned to adenine dimers or to high-energy tautomers since higher oven temperatures result in higher adenine pressures in the scattering-box oven and thus a greater probability for picking up more than one molecule.[15] However, as discussed in a previous paper,[15] higher-energy tautomers are also favored at higher temperatures, so that a definitive assignment of these bands will have to await a more detailed investigation in which the vapor pressure of the sample in the pick-up cell can be varied independently of the temperature.

As listed in Table 1, the ab initio VTMA for the N9H band at 3509.2 cm^{-1} is 59°, in good agreement with the experimental value, namely, 63°. Similarly, the bands in the region of 3504−3508 cm^{-1} are assigned to the adenine dimers or high-energy tautomers. The band at 3509.2 cm^{-1} has a temperature dependence that is consistent with the pick-up of a single molecule by the droplets. The oven temperature dependence of the intensities of the NH_2 (SS) and N9H bands in Figure 4 is discussed in the Supporting Information.

We now turn our attention to the region of the spectrum corresponding to the NH_2 (AS) vibrational band at 3568.2 cm^{-1}. Quantitative analysis of this band gives experimental VTMAs of 24°, which is in excellent agreement with the ab initio value, 21°.

Up to now, we have shown that the combination of the ab initio frequencies and the VTMA assignment of each vibrational band of the global minimum structure of adenine, A9, gives a conclusive assignment of the adenine monomer. Now, we begin

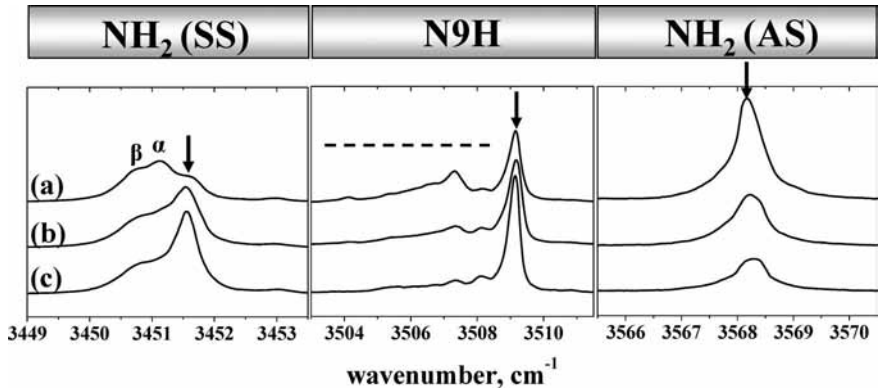

Figure 4. Expanded views of each vibrational band region of the adenine spectrum. Spectra (a), (b), and (c) correspond to parallel polarization, zero-field, and perpendicular polarization, respectively. The bands marked with the downward point arrows are assigned to the NH_2 (SS), N9H, and NH_2 (AS) modes of A9. The bands marked with an "α" and a "*β*" in NH_2 (SS) and in the range of 3504−3508 cm^{-1} marked with a dash line are due to the adenine dimer or higher-energy tautomers.

discussing the issue of adenine nonplanarity. It is well-known that the VTMAs of vibrational modes are very stable to basis set size compared to the stability of ab initio frequencies of each vibrational band upon different basis sets.[12] Furthermore, the calculated harmonic frequencies have to be scaled to correct for the anharmonicity; however, the calculated VTMAs are essentially independent of a basis set size, suggesting that quantitative comparisons can be made with experiment even using very modest ab initio calculations. This is important when applying these techniques to much larger systems, where large basis sets may be prohibitively expensive. The reason for the insensitivity of the VTMAs to basis set size can be appreciated by noting that, for the localized vibrations considered here, the transition moment directions are primarily determined by bond directionality.[12] Therefore, as long as the calculated structure is good, the directions of the permanent and transition moments will be rather well determined.

The nonplanarity of the A9 tautomer is reflected in the dihedral angles of $N^1C^6N^{10}H^{14}$, $N^1C^6N^{10}H^{15}$, and $C^2N^1C^6N^{10}$ (see Figure 1). Therefore, we have conducted an extensive study of the evolution of the other two dihedral angles, namely, $N^1C^6N^{10}H^{15}$ and $C^2N^1C^6N^1$, of the A9 tautomer as a function of $N^1C^6N^{10}H^{14}$ from 0 to 40° using a B3LYP and MP2 level of theory with a cc-pVDZ basis set, shown in Figure 5a and c, respectively. The calculations were conducted by freezing the dihedral angle, $N^1C^6N^{10}H^{14}$, while all of the others were fully relaxed. The result shows that the A9 tautomer is planar when $N^1C^6N^{10}H^{14}$ is zero, which is independent of the level of theory used in this study. However, at the fully relaxed geometry optimization of the A9 tautomer, the B3LYP and MP2 levels of theory resulted in a planar and nonplanar structure of a dihedral angle ($N^1C^6N^{10}H^{14}$) of 0 and 20°, marked with a vertical line in Figure 5b and d, respectively. The different horizontal lines (dotted, dashed, and dot−dashed) indicate the experimental VTMAs of the vibrational bands of the A9 tautomer, NH_2 (AS), N9H, and NH_2 (SS), respectively. Figure 5d shows that the experimental VTMAs are in excellent agreement with the ab initio values done with the MP2 calculations. It is worth pointing out that the A9 tautomer is constrained to be planar when the dihedral angle of the $N^1C^6N^{10}H^{14}$ is fixed to 0° with the MP2 level of theory, which is very similar to the result with the B3LYP method. The VTMAs of the three vibrational modes with a full optimization with the MP2 level can also be reproduced by constraining the dihedral angle $N^1C^6N^{10}H^{14}$ of the planar adenine to 20° with a B3LYP method. Taking all of

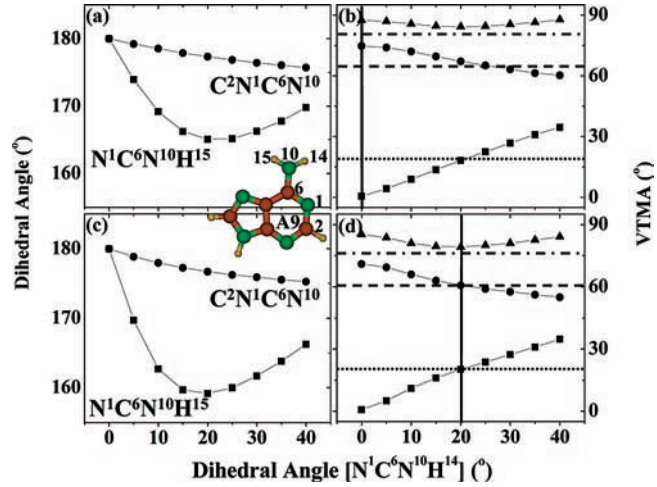

Figure 5. The evolution of the dihedral angles (a and c) and VTMAs (b and d) of the A9 tautomer as a function of the dihedral angle, $N^1C^6N^{10}H^{14}$, from 0 to 40°, using a cc-pVDZ basis set with B3LYP (a and b) and MP2 (c and d) levels of theory. The vertical line in (b) and (d) shows that the dihedral angles, $N^1C^6N^{10}H^{14}$, of the optimized structure of A9 are 0 and 20° with the B3LYP and MP2 levels of theory using a cc-pVDZ basis set, respectively. The different horizontal lines (dotted, dashed, and dot−dashed) indicate the experimental VTMAs of the vibrational bands of the A9 tautomer, NH_2 (AS), N9H, and NH_2 (SS), respectively.

the experimental and theoretical data presented above together, it is certain that the NH_2 group is not in the plane of the purine ring.

It is very interesting to note that the geometries of adenine show a large dependence on the type of theory used, namely, the MP2 and B3LYP methods. However, the evolution of VTMAs of all three vibrational bands shown in Figure 5b and d shows almost no difference depending on the level of theory used in this study. This is, while the MP2 and DFT calculations may disagree about the planarity of adenine, they both agree about the values of the VTMAs at their nonplanar geometry of adenine. This further supports that VTMA is very sensitive to the structure of the molecules.

Similarly, Figure 6 shows the evolution of the dihedral angles, $N^1C^6N^{10}H^{15}$ and $C^2N^1C^6N^1$, and VTMAs of each vibrational band of the A7 (a and b) and A3 (c and d) tautomers as a function of $N^1C^6N^{10}H^{14}$ from 0 to 40° using the MP2 level of theory with a cc-pVDZ basis set. The vertical line in Figure 6b

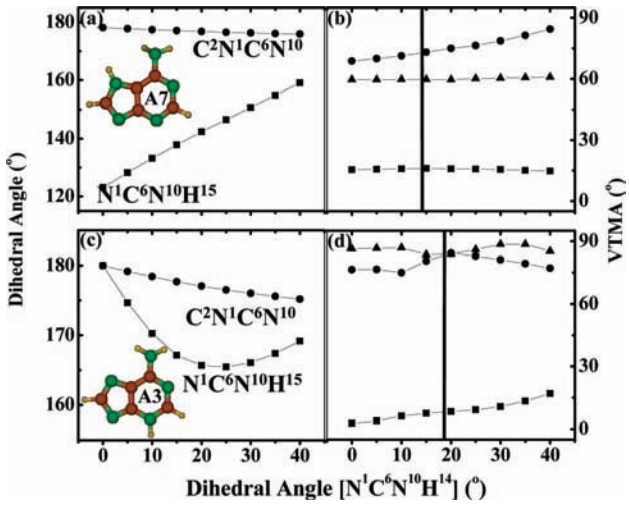

Figure 6. The evolution of the dihedral angles (a and c) and VTMAs (b and d) of the A7 and A3 tautomer as a function of the dihedral angle, $N^1C^6N^{10}H^{14}$, from 0 to 40° using a cc-pVDZ basis set with the MP2 level of theory. The vertical line in (b) and (d) shows that the dihedral angle, $N^1C^6N^{10}H^{14}$, of the optimized structure of A7 and A3 is 14 and 18°, respectively.

and d is the dihedral angle of the optimized structure of each tautomer, 14 and 18°, respectively. It is worth noting that the A7 tautomer shown in Figure 6a is not planar not only at the dihedral angle, $N^1C^6N^{10}H^{14}$, of 0° but also with the B3LYP/cc-pVDZ calculations. This could be attributed to the steric hindrance caused by N7H close to the NH_2 group.

Summary

In this combined experimental/theoretical study, we have presented the infrared laser spectroscopic investigation of adenine isolated in helium nanodroplets. By using ab initio frequency/vibrational transition moment angle (VTMA) calculations and the measurement of VTMAs for each vibrational stretching mode, we have observed only the global minimum structure of adenine (A9) in helium droplets. The vibrational bands of higher-order clusters or high-energy tautomers of adenine were identified by the temperature dependence experiments. However, specific assignments of the bands are beyond the scope of this study.

Most interestingly, the experimental VTMAs of each vibrational band matched with the ab initio values obtained from a nonplanar structure geometry of the global minimum structure of adenine (A9). The nonplanarity of A9 has been further confirmed by studying the evolution of the VTMAs of each vibrational mode as the dihedral angle, $N^1C^6N^{10}H^{14}$, is changed. A detailed VTMA study of two more tautomers, A7 and A3, has also been conducted, resulting in both having a nonplanar structure. Further studies of the nonplanarity of the two tautomers suggest that only A7 among the amino tautomers of adenine (shown in Figure 1) exhibits a nonplanar structure even at the dihedral angle, $N^1C^6N^{10}H^{14}$, of 0°. We hope that this study gives more insights for further experimental and theoretical studies on adenine.

Acknowledgment. This work was supported by the Korea Research Foundation Grant funded by the Korean Government (MOEHRD, Basic Research Promotion Fund) (KRF-313-C00339). M.Y.C. appreciates the University of North Carolina at Chapel Hill and KISTI supercomputing center for the computer sources used in the ab initio calculations reported here and the Young Faculty Research Fund at GNU. The authors are grateful to Prof. Tomas Baer for careful reading of the manuscript.

Supporting Information Available: Figure of the oven temperature dependence of the intensities of the NH_2 (SS) and N9H stretch band region shown in Figure 4. This material is available free of charge via the Internet at http://pubs.acs.org.

References and Notes

(1) Watson, J. D.; Crick, F. H. C. *Nature* **1953**, *171*, 737.
(2) Weinkauf, R.; Schermann, J. P.; De Vries, M. S.; Kleinermanns, K. *Eur. Phys. J. D* **2002**, *20*, 309.
(3) Aamouche, A.; Ghomi, M.; Grajcar, L.; Baron, M. H.; Romain, F.; Baumruk, V.; Stepanek, J.; Coulombeau, C.; Jobic, H.; Berthier, G. *J. Phys. Chem. A* **1997**, *101*, 10063.
(4) Hobza, P.; Sponer, J. *Chem. Rev.* **1999**, *99*, 3247.
(5) Shishkin, O. V.; Gorb, L.; Hobza, P.; Leszczynski, J. *Int. J. Quantum Chem.* **2000**, *80*, 1116.
(6) Sponer, J.; Hobza, P. *J. Phys. Chem.* **1994**, *98*, 3161.
(7) Sponer, J.; Hobza, P. *J. Am. Chem. Soc.* **1994**, *116*, 709.
(8) Sponer, J.; Leszczynski, J.; Hobza, P. *J. Mol. Struct.: THEOCHEM* **2001**, *573*, 43.
(9) Kung, H. C.; Wang, K. Y.; Goljer, I.; Bolton, P. H. *J. Magn. Reson., Ser. B* **1995**, *109*, 323.
(10) Luisi, B.; Orozco, M.; Sponer, J.; Luque, F. J.; Shakked, Z. *J. Mol. Biol.* **1998**, *279*, 1123.
(11) Godfrey, P. D.; McNaughton, D.; Pierlot, A. P. *Chem. Phys. Lett.* **1989**, *156*, 61.
(12) Dong, F.; Miller, R. E. *Science* **2002**, *298*, 1227.
(13) Douberly, G. E.; Miller, R. E. *J. Phys. Chem. B* **2003**, *107*, 4500.
(14) Choi, M. Y.; Miller, R. E. *Phys. Chem. Chem. Phys.* **2005**, *7*, 3565.
(15) Choi, M. Y.; Dong, F.; Miller, R. E. *Philos. Trans. R. Soc. London, Ser. A* **2005**, *363*, 393.
(16) Choi, M. Y.; Miller, R. E. *J. Am. Chem. Soc.* **2006**, *128*, 7320.
(17) Choi, M. Y.; Miller, R. E. *J. Phys. Chem. A* **2006**, *110*, 9344.
(18) Choi, M. Y.; Miller, R. E. *J. Phys. Chem. A* **2007**, *111*, 2475.
(19) Choi, M. Y.; Douberly, G. E.; Falconer, T. M.; Lewis, W. K.; Lindsay, C. M.; Merritt, J. M.; Stiles, P. L.; Miller, R. E. *Int. Rev. Phys. Chem.* **2006**, *25*, 15.
(20) Nauta, K.; Miller, R. E. *J. Chem. Phys.* **1999**, *111*, 3426.
(21) Lehmann, K. K.; Scoles, G. *Science* **1998**, *279*, 2065.
(22) Toennies, J. P.; Vilesov, A. F. *Angew. Chem., Int. Ed.* **2004**, *43*, 2622.
(23) Stienkemeier, F.; Lehmann, K. K. *J. Phys. B: At. Mol. Opt. Phys.* **2006**, *39*, R127.
(24) Gough, T. E.; Mengel, M.; Rowntree, P. A.; Scoles, G. *J. Chem. Phys.* **1985**, *83*, 4958.
(25) Hartmann, M.; Miller, R. E.; Toennies, J. P.; Vilesov, A. F. *Phys. Rev. Lett.* **1995**, *75*, 1566.
(26) Brink, D. M.; Stringari, S. *Z. Phys. D: At., Mol. Clusters* **1990**, *15*, 257.
(27) Schneider, K.; Kramper, P.; Schiller, S.; Mlynek, J. *Opt. Lett.* **1997**, *22*, 1293.
(28) Schneider, K.; Kramper, P.; Mor, O.; Schiller, S.; Mlynek, J. *OSA Trends Opt. Photonics Ser.* **1998**, *19 (Advanced Solid State Lasers)* , 256.
(29) Gough, T. E.; Miller, R. E.; Scoles, G. *Appl. Phys. Lett.* **1977**, *30*, 338.
(30) Block, P. A.; Bohac, E. J.; Miller, R. E. *Phys. Rev. Lett.* **1992**, *68*, 1303.
(31) Moore, D. T.; Oudejans, L.; Miller, R. E. *J. Chem. Phys.* **1999**, *110*, 197.
(32) Wu, M.; Bemish, R. J.; Miller, R. E. *J. Chem. Phys.* **1994**, *101*, 9447.
(33) Bemish, R. J.; Chan, M. C.; Miller, R. E. *Chem. Phys. Lett.* **1996**, *251*, 182.
(34) Jucks, K. W.; Miller, R. E. *J. Chem. Phys.* **1987**, *87*, 5629.
(35) Nauta, K.; Miller, R. E. *Phys. Rev. Lett.* **1999**, *82*, 4480.
(36) Nauta, K.; Miller, R. E. *Science* **1999**, *283*, 1895.
(37) Nauta, K.; Moore, D. T.; Stiles, P. L.; Miller, R. E. *Science* **2001**, *292*, 481.
(38) Franks, K. J.; Li, H. Z.; Kong, W. *J. Chem. Phys.* **1999**, *110*, 11779.
(39) Castle, K. J.; Abbott, J.; Peng, X.; Kong, W. *J. Chem. Phys.* **2000**, *113*, 1415.
(40) Kong, W.; Bulthuis, J. *J. Phys. Chem. A* **2000**, *104*, 1055.
(41) Callegari, C.; Lehmann, K. K.; Schmied, R.; Scoles, G. *J. Chem. Phys.* **2001**, *115*, 10090.
(42) Michael, S.; Sid, T.; William, C. L. *J. Phys. Chem.* **1990**, *94*, 1366.
(43) Gu, J. D.; Leszczynski, J. *J. Phys. Chem. A* **1999**, *103*, 2744.

(44) Huang, Y.; Kenttamaa, H. *J. Phys. Chem. A* **2004**, *108*, 4485.
(45) Hanus, M.; Kabelac, M.; Rejnek, J.; Ryjacek, F.; Hobza, P. *J. Phys. Chem. B* **2004**, *108*, 2087.
(46) Frisch, M. J. Trucks, G. W.; Schlegel, H. B.; Scuseria, G. E.; Robb, M. A.; Cheeseman, J. R.; Montgomery, J. A., Jr.; Vreven, T.; Kudin, K. N.; Burant, J. C.; Millam, J. M.; Iyengar, S. S.; Tomasi, J.; Barone, V.; Mennucci, B.; Cossi, M.; Scalmani, G.; Rega, N.; Petersson, G. A.; Nakatsuji, H.; Hada, M.; Ehara, M.; Toyota, K.; Fukuda, R.; Hasegawa, J.; Ishida, M.; Nakajima, T.; Honda, Y.; Kitao, O.; Nakai, H.; Klene, M.; Li, X.; Knox, J. E.; Hratchian, H. P.; Cross, J. B.; Bakken, V.; Adamo, C.; Jaramillo, J.; Gomperts, R.; Stratmann, R. E.; Yazyev, O.; Austin, A. J.; Cammi, R.; Pomelli, C.; Ochterski, J. W.; Ayala, P. Y.; Morokuma, K.; Voth, G. A.; Salvador, P.; Dannenberg, J. J.; Zakrzewski, V. G.; Dapprich, S.; Daniels, A. D.; Strain, M. C.; Farkas, O.; Malick, D. K.; Rabuck, A. D.; Raghavachari, K.; Foresman, J. B.; Ortiz, J. V.; Cui, Q.; Baboul, A. G.; Clifford, S.; Cioslowski, J.; Stefanov, B. B.; Liu, G.; Liashenko, A.; Piskorz, P.; Komaromi, I.; Martin, R. L.; Fox, D. J.; Keith, T.; Al-Laham, M. A.; Peng, C. Y.; Nanayakkara, A.; Challacombe, M.; Gill, P. M. W.; Johnson, B.; Chen, W.; Wong, M. W.; Gonzalez, C.; Pople, J. A. *Gaussian 03*, revision C.02; Gaussian, Inc.: Wallingford, CT, 2004.

JP8012688